Design and Fabrication of a Biodegradable, Covalently Crosslinked Shape-Memory Alginate Scaffold for Cell and Growth Factor Delivery

Lin Wang, Ph.D.,[1,2] Janet Shansky, M.Sc.,[3] Cristina Borselli, Ph.D.,[2]
David Mooney, Ph.D.,[2] and Herman Vandenburgh, Ph.D.[2–4]

The successful use of transplanted cells and/or growth factors for tissue repair is limited by a significant cell loss and/or rapid growth factor diffusion soon after implantation. Highly porous alginate scaffolds formed with covalent crosslinking have been used to improve cell survival and growth factor release kinetics, but require open-wound surgical procedures for insertion and have not previously been designed to readily degrade *in vivo*. In this study, a biodegradable, partially crosslinked alginate scaffold with shape-memory properties was fabricated for minimally invasive surgical applications. A mixture of high and low molecular weight partially oxidized alginate modified with RGD peptides was covalently crosslinked using carbodiimide chemistry. The scaffold was compressible 11-fold and returned to its original shape when rehydrated. Scaffold degradation properties *in vitro* indicated ∼85% mass loss by 28 days. The greater than 90% porous scaffolds released the recombinant growth factor insulin-like growth factor-1 over several days *in vitro* and allowed skeletal muscle cell survival, proliferation, and migration from the scaffold over a 28-day period. The compressible scaffold thus has the potential to be delivered by a minimally invasive technique, and when rehydrated *in vivo* with cells and/or growth factors, could serve as a temporary delivery vehicle for tissue repair.

Introduction

MANY APPROACHES FOR treating tissue injuries such as that occur during skeletal muscle trauma involve attempts to incorporate stem cells to the damaged area to regenerate new tissue.[1,2] However, direct cell injections have been unsuccessful because of the rapid loss in the viability of the majority of the cells.[3,4] Thus, to restore the structure and the function of injured tissues such as skeletal muscle, a more effective cell transplantation method is of great interest, with the aim of prolonging the survival of implanted cells, while maintaining their functionality and enhancing their incorporation into the host tissue. One strategy to achieve this goal is to deliver transplanted cells via a scaffold made of biocompatible materials that are biochemically and physically modified to optimize the above aims.

Various biomaterials have been developed for the use as synthetic scaffolds for tissue regeneration. One example is alginate, a tunable and versatile biomaterial that has been used in many medical applications, including cell transplantation, drug delivery, and wound dressing.[5] An ionically crosslinked, highly porous alginate scaffold previously developed by Hill *et al.*

improved transplanted myoblast repopulation and significantly enhanced damaged muscle regeneration in a mouse laceration model.[1] However, the scaffold was introduced to the injury site via an invasive open surgical procedure. Bouhadir *et al.*[6] have developed a covalently crosslinked, highly porous alginate scaffold with shape memory, the capacity to be highly compressed and recover its original shape in response to an environmental stimulus.[7,8] This type of shape-memory scaffold possesses the structure-defining property of implantable materials, while allowing for a minimally invasive method of implantation. The less traumatic introduction of the implant into the body may lead to reduced pain and accelerated recovery. In a study by Thornton *et al.*, macroporous alginate hydrogel scaffolds were prepared in predefined geometries, dehydrated, and compressed into small, temporary forms.[9] When rehydrated *in vitro* with a suspension of cells, the scaffolds rapidly returned to their original shape, suggesting that they might be suitable for minimally invasive implantation.[9,10] In a follow-on study, the dehydrated scaffolds were delivered *in vivo* and rehydrated *in situ* with a saline containing bovine chondrocytes. Explants showed that the scaffolds had recovered their original shape and size and facilitated new tissue

---

[1]Department of Molecular Pharmacology, Physiology, and Biotechnology, Brown University, Providence, Rhode Island.
[2]School of Engineering and Applied Sciences, Harvard University, Cambridge, Massachusetts.
[3]Myomics, Inc., Providence, Rhode Island.
[4]Department of Pathology, Brown Medical School, Providence, Rhode Island.

formation with the geometry of the original scaffold.[9] However, this type of covalently crosslinked shape-memory scaffold had an extremely slow degradation rate, with 80% of the scaffolds maintaining their original three-dimensional (3D) shape[10] after 6 months *in vivo*. This is a critical limitation for a tissue-engineering material, as surgery would be required to remove the implant. It would be desirable for the degradation rate of the implanted material to match the rate of new tissue formation, ~4–6 weeks in the case of skeletal muscle.[11]

The major goal of this study was to design and fabricate a scaffold with the following characteristics: shape-memory properties for facilitation of minimally invasive implantation; a degradation rate with the same time frame as new tissue formation; and a surface structure to support optimal affinity of seeded cells. In addition, the scaffold should have the capacity to release incorporated growth factors to aid in tissue repair. We generated a scaffold with these characteristics by modifications to previous alginate scaffold formulations, using irradiation to generate low molecular weight (LMW) alginate, oxidation for increased biodegradability, and RGD modification to improve cell adhesion. Scaffold materials were evaluated for shape-memory properties, including swelling ratio and porosity, degradation rate, cell survival and migration, and release kinetics of a growth factor (insulin-like growth factor-1 [IGF-1]) incorporated into the scaffold.

Our results show that the shape-memory alginate scaffold developed has the potential to serve as a synthetic matrix for regeneration of damaged tissue such as skeletal muscle.

Materials and Methods

Fabrication of alginate scaffolds

The LMW alginate was generated by gamma irradiation of high molecular weight (HMW) LF 20/40 alginate (FMC Biopolymer, Philadelphia, PA) at 5.0 Mrad for 4 h with a cobalt-60 source.[12] To fabricate oxidized alginates, both LMW and HMW alginates were diluted to 1% w/v in ddH$_2$O, and 1%, 5%, or 10% of the sugar residues (uronic groups) were oxidized by using different amounts of sodium periodate (Sigma-Aldrich, St. Louis, MO). Solutions were maintained in the dark for 19 h at room temperature, and an equimolar volume of ethylene glycol (Fisher Scientific, Fair Lawn, NJ) was added to quench the reaction. The solutions were then dialyzed using Spectra/Por dialysis tubing (VWR International, Pittsburgh, PA), filtered, and lyophilized to generate 1%, 5%, and 10% oxidized LMW and HMW alginates.[13]

All alginate components were further modified with a linear RGD peptide (G$_4$RGDSP-OH; Commonwealth Biotechnology, Inc., Richmond, VA) using 1-ethyl-(dimethyl aminopropyl) carbodiimide N-hydroxysulfosuccinimide (Sigma-Aldrich), as previously described.[14]

To prepare covalently crosslinked alginate scaffolds, sodium alginate 2% (w/v) was first dissolved in an MES buffer [0.1 M 2-(N-morpholino) ethanesulfonic acid; 0.3 M NaCl; Sigma-Aldrich], pH 6.0. Covalently crosslinked hydrogels were formed by the standard carbodiimide chemistry using 1-ethyl-(dimethyl aminopropyl) carbodiimide, 1-hydroxybenzotriazole, and the bifunctional crosslinker adipic acid dihydrazide (AAD; Sigma-Aldrich) (ratio of AAD: reactive groups on polymer, 1:20), as previously described.[15] Scaf-

folds were then placed in a large volume of distilled water for a minimum of 24 h to attain equilibrium swelling and to remove residual unpolymerized chemicals.

Three different scaffolds were fabricated as follows, each with LMW and HMW alginate combined in a 1:1 weight ratio:

A. 1% binary group: 1% oxidized HMW alginate × 1% oxidized LMW alginate

B. 5% binary group: 5% oxidized HMW alginate × 5% oxidized LMW alginate

C. 10% binary group: 10% oxidized HMW alginate × 10% oxidized LMW alginate

The resulting alginate materials were frozen at −20°C and lyophilized to generate macroporous scaffolds with variable pore characteristics.[16]

Scaffold degradation and swelling measurements

Scaffold degradation was evaluated under *in vitro* physiologic conditions in DPBS (Gibco, Grand Island, NY). Scaffolds were fabricated sterilely, cut into squares (5 mm × 5 mm), and immersed in 10-mL glass tubes with 3 mL of sterile DPBS (containing Ca^{2+} and Mg^{2+}), 1% pen/strep, and 1% fungizone (Invitrogen, Carlsbad, CA).

The tubes were fixed on a tube rack on a belly-dancer shaker set to rotate at a constant speed (0.33 rpm) at a fixed 15° angle to simulate a mechanically active *in vivo* environment. The shaker was placed in a 37°C, 5% CO$_2$ incubator, and scaffold degradation was monitored over 6 weeks. At each time point (1, 2, 4, 12, 21, and 39 days), the tubes were removed, and the liquid phase was aspirated carefully. The bulky, solid phase of the scaffolds remaining in the tubes was lyophilized and considered as the dry weight of the undissolved scaffold at that time point, and the mass of the fine particulate matter in the liquid phase was also lyophilized and considered as partially degraded scaffold. The percent of weight loss was calculated, and the percent of scaffold mass loss was graphed as a function of time. The degradation here refers to disassembly of the scaffold, that is, the breakage of the crosslink between polymers, but not polymer backbone degradation; the weight of the suspended fine particulate material in aqueous solution was not included as a remaining scaffold weight. The fine particulate was considered the degraded part from the bulk of the alginate scaffold because of its low weight (≤0.5 mg).

Scaffold porosity (void volume), pore characteristics, and equilibrium swelling ratios (Qs) were determined following previously published protocols.[15,17] Scaffold dimensions were measured with Vernier calipers, lyophilized, and then rehydrated with distilled water to determine their ability to return to their original dimensions. The scaffold swelling ratio was quantified by first compressing the lyophilized 5% oxidized 1LMW:1HMW scaffolds at 500 psi to a thin layer (0.12 mm in depth) and then by rehydrating the scaffold with distilled water until equilibrium. The porosity and swelling ratio were calculated from the weight before and after rehydration. The initial wet weight of the rehydrated scaffolds (W_S) was recorded, and the scaffold dry weight (W_D) was determined after lyophilization. The scaffold swelling ratio (QS) was calculated as the mass ratio of absorbed water to dry weight, calculated from $QS = (W_S − W_D)/W_D$. At least, three samples were tested at each time point. Porosity was calculated as $(W_S − W_D)/W_S$.

SEM of scaffold surface

The surface morphology was analyzed by SEM. The lyophilized scaffolds were placed on the surface of a carbon adhesive paper and coated with gold nanoparticles by a sputter coater to make the surface conductive. Default settings used for coating were 4 min, 25 mA, one coating for each sample. Images were taken by a HITACHI 2700 Scanning Electron Microscope (voltage: 6KV/beam current: 6*/scanning speed: 160). The images were collected with a Quartz PCI digital imaging system (Quartz Imaging Corporation, Vancouver, BC Canada) and analyzed with ImageJ software (NIH).

Measurement of cell distribution, migration, and proliferation

For measurement of cell distribution on scaffolds, primary mouse myoblasts stably transduced to express GFP (PMMGFP) were expanded in culture, and each scaffold was plated with 300,000 cells. The cells were suspended in 50 μL primary mouse myoblast growth medium (PMMGM: 20% fetal bovine serum [Gibco], 39% Dulbecco's modified Eagle's medium [DMEM; Gibco], 39% fibroblast growth medium [Lonza, Walkersville, MD], 1% ITS liquid medium supplement [Sigma-Aldrich], and 1% penicillin/ streptomycin [Sigma-Aldrich]) and pipetted dropwise onto the scaffolds in 35-mm-diameter tissue culture dishes. The dishes were placed for 30 min in a 5% CO_2 humidified incubator at 37°C before being covered with 1 mL PMMGM to immerse the scaffolds. The medium was changed daily. Images were taken 2 weeks after the cells were seeded onto the scaffolds with a Leica TCS SP2 AOBS spectral confocal microscope. Images were acquired and analyzed with Leica confocal software (LCS) version 2.5.

Cell viability and migration were also measured using PMMGFP cells (P.H. Lee and H. Vandenburgh, unpublished data). Five percent oxidized covalently crosslinked 1LMW:1HMW scaffolds were prepared sterilely, cut into squares ($5 \times 5 \times 2$ mm^3 when hydrated), and lyophilized. PMMGFP cells were expanded in the PMMGM and harvested as described above. A suspension containing 0.3 million cells in 50 μL of DMEM was pipetted onto each scaffold. The scaffolds were transferred into the wells of a 24-well collagen-coated plate and allowed to sit undisturbed for 30 min, and then 250 μL of growth medium was added to each well and the plate transferred to a humidified 37°C CO_2 incubator. To measure migration of cells from the scaffolds, the cell-seeded scaffolds were transferred to new 24-well plates every 24 h, and the cells that had attached to the 24-well plates over the previous 24 h were trypsinized and counted with trypan blue staining. The total number of cells that were trypsinized every 24 h from the surface of the plate after removal of the scaffold was considered as the cells that had migrated off the scaffold. The number of cells that migrated off every 24 h was totaled and considered the accumulated number of cells that had migrated by each time point. The migration analysis was repeated a second time using a different batch of PMMGFP cells. The number of viable cells inside the scaffolds 2 h after seeding was used as the initial cell number, and cell viability and migration were determined at the following time points: 24 h, 48 h, 72 h, 96 h, 1 week, 2 weeks, and 3 weeks.

Cell proliferation on the scaffolds was determined by quantifying the intensity of the GFP protein extracted from the cells remaining on the scaffolds, as previously described.[18] Briefly, cells on the scaffolds were lysed, and the total protein was extracted by incubating the cell–scaffold construct in 1 mL radioimmuno precipitation assay (RIPA) on ice for 20 min. The lysate was centrifuged at 14,000g at 4°C for 15 min and the supernatant transferred to a fresh centrifuge tube, and samples were diluted 100-fold for measurement of extracted GFP. The GFP intensity was measured in duplicate on 200-μL samples with a Synergy HT microplate reader (Biotek, Winooski, VT) set at excitation 485 nm and emission 528 nm. The background GFP intensity was measured from a blank scaffold (no cells) processed, as described above. The amount of GFP increases linearly with the cell number and is an accurate assay for quantifying viable GFP cells.[18–20] A standard curve was plotted for the relative GFP intensity versus a known number of GFP-transduced cells, and the number of viable GFP cells in each scaffold was then determined from the relative GFP intensity of the extracted scaffold samples.

IGF-1 release assay

An IGF-1 solution was prepared in DPBS, incorporated into square scaffolds ($5 \times 5 \times 2$ mm^3 when hydrated) by two different methods, and the release kinetics of these methods compared.

Method A. Lyophilized 5% 1LMW:1HMW scaffolds (5 mm × 5 mm × 2 mm) were rehydrated with 50 μL of an IGF-1 solution (60 μg/mL), then frozen, and lyophilized again.

Method B. Lyophilized 5% 1LMW:1HMW scaffolds (5 mm × 5 mm × 2 mm) were rehydrated with 50 μL of an IGF-1 solution (60 μg/mL) and used directly in the IGF-1-release studies.

The IGF-1-containing scaffolds prepared by both methods were transferred to 1.5-mL polypropylene tubes (one scaffold per tube) containing 1 mL of DPBS and incubated in a water bath at 37°C. After 24 h, 48 h, 72 h, 1 week, 2 weeks, and 3 weeks, the tubes were centrifuged, and the supernatant was transferred to a new sterile tube. Fresh DPBS was then added to the tubes containing the scaffolds, and they were again placed in the water bath at 37°C until the next time point. All supernatant samples were stored at −80°C.

The release kinetics of IGF-1 from the scaffolds was determined by ELISA (Quantikine Human IGF-I Immunoassay; R&D Systems, Minneapolis, MN), following the manufacturer's protocol. The absorbance of each sample was measured at 450 nm and corrected at 540 nm with a Synergy HT microplate reader. A standard curve was plotted for absorbance versus IGF-1 concentration (ranging from 0.094 to 6 ng/mL), and the concentration of IGF-1 in experimental samples was read from the curve.

Results

Scaffold degradation

The extremely slow degradation rate of covalently crosslinked scaffolds made exclusively from high molecular weight alginate[10] limits their use in a biomaterial-mediated
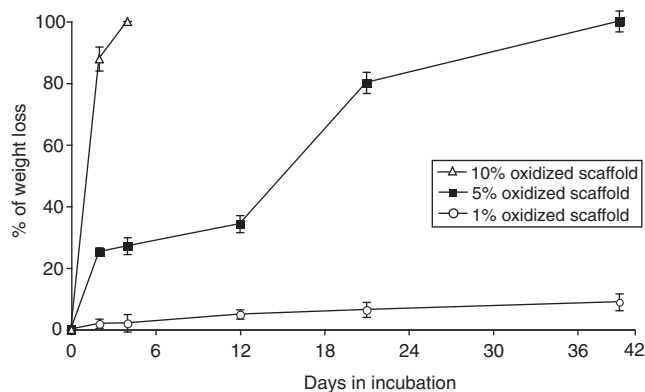
FIG. 1. The percentage of weight loss over time for covalently crosslinked scaffolds fabricated with a 1:1 ratio of low molecular weight:high molecular weight (LMW:HMW) alginate and different extents of oxidation as described in the Materials and Methods section.

in vivo repair treatment. LMW alginate (MW < 50 kDa) can be passed by the kidneys *in vivo*, and thus can be cleared by the renal system,[21] whereas HMW alginate cannot be cleared. To improve the degradation rate, we introduced several combinations of modifications, including irradiation to produce LMW alginate, oxidation of both LMW and HMW alginates to promote susceptibility to hydrolysis, and control over molecular weight distribution of the polymers used to form the gels.

Specifically, the HMW and LMW alginate components were oxidized to a theoretical extent of 1%, 5%, 10%, and the oxidized components were then combined to form alginate hydrogels with a 1:1 weight ratio of a HMW and LMW polymer.

As illustrated in Figure 1, 10% 1LMW:1HMW scaffolds degrade *in vitro* at the fastest rate, with complete degradation observed by day 4. In contrast, the degradation rate for 1% 1LMW:1HMW scaffolds was slowest, with ~10% weight lost by day 39. However, the 5% 1LMW:1HMW scaffolds had ~34% average weight loss by day 12 and 100% by day 39 (Table 1 and Fig. 1). Based on these results, the 5% 1LMW:1HMW scaffolds had a degradation profile that most closely matches the natural regeneration time frame of damaged skeletal muscle, and therefore were selected for further study.

Characterization of shape-memory properties

Shape-memory properties largely determine whether or not the scaffold can be delivered by a minimally invasive method. We evaluated the ability of the 5% 1LMW:1HMW scaffold to

TABLE 1. AVERAGE WEIGHT LOSS OF COVALENTLY CROSSLINKED SCAFFOLDS WITH DIFFERENT EXTENTS OF OXIDATION

Crosslink density	D0	D2	D4	D12	D21	D39
1% 1:1LMW:HMW	0	1.8%	2.0%	4.8%	6.4%	8.8%
5% 1:1LMW:HMW	0	25.1%	27.1%	34.2%	80.1%	100.0%
10% 1:1LMW:HMW	0	87.3%	100.0%			

LMW:HMW, low molecular weight:high molecular weight.

TABLE 2. SHAPE-MEMORY PARAMETERS OF 5% OXIDIZED 1LMW:1HMW SCAFFOLD

Crosslink density	Porosity	Swelling ratio	% of volume recovered
Original scaffold	98.1% ± 0.1%	56.2 ± 2.2	90.0% (compressed manually)
5% 1LMW: 1HMW	90.7% ± 0.3%	11.36 ± 0.2	80.6% (compressed at 500 psi)

The unmodified HMW covalently crosslinked shape-memory scaffold was developed by Thornton *et al.* (9) and compressed manually. Data represent mean ± standard error of the mean (*n* = 4).

retain the shape and dimensions by measuring the dimensions of the scaffold before and after rehydration, and calculated two main shape-memory properties: swelling ratio and porosity. Results were compared to an unmodified HMW scaffold previously developed by Thornton *et al.*[9] (Table 2). The percentage of volume recovery was determined by the volume of the rehydrated scaffolds compared to the initial swollen gel volume before lyophilization. Strikingly, the average swelling ratio of the 5% 1LMW:1HMW scaffold was ~11, indicating that the scaffold can swell to ~11 times its compressed volume after rehydration. The porosity was measured at ~90.7%, implying that the scaffolds are highly porous and have high water content in interconnected large pores (~90%). These data indicate that the scaffolds made with a 1:1 ratio of 5% oxidized LMW and 5% oxidized HMW alginate maintained good shape-memory properties. They also appear to have high porosity, which may be beneficial for cell uptake.

Scaffold surface porosity and cell distribution

Scaffolds with high porosity offer a structural advantage for the use as a vehicle in delivery of cells for various repair and bioengineering applications. To assess porosity of the 5% 1LMW:1HMW scaffold, we imaged their surface using a scanning electron microscope.[22] As illustrated in Figure 2a, the scaffolds were extremely porous with an average pore size of 412 μm, which falls into the optimal scaffold pore size range of between 100 and 500 μm for cell growth.[23] The 3D porous structure of the scaffold remains after the scaffold is rehydrated. The cells gather at the pores of the scaffold when they are first
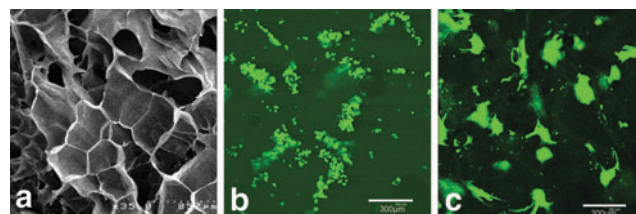

FIG. 2. SEM imaging of the lyophilized porous 5% 1LMW:1HMW scaffold **(a)** and confocal imaging of primary mouse myoblasts stably transduced to express GFP (PMMGFP) growing on the RGD modified 5% 1LMW:1HMW scaffold 30 min after seeding **(b)** and after 2 weeks in culture **(c)**. The average pore size is 400 ± 20 μm. Data represent mean ± standard error of the mean (*n* = 4). Color images available online at www.liebertpub.com/tea

FIG. 3. Light microscopy of myoblast clusters (indicated by white arrows) growing in the scaffold pores 2 weeks after seeding **(a)**. Scaffold area is outlined with dashed white lines. Cells both migrated out of the scaffold 2 weeks after they were initially seeded **(b, c)**, and continued to grow (cells indicated with white arrow heads) on the plate surface **(d)**. About 0.3×10^6 PMMGFP cells were initially seeded on the 5% 1LMW:1HMW scaffolds and maintained under cell culture conditions as described in the Methods. Images are taken at $200 \times$ with a Nikon e600 microscope equipped with a DP70 Camera. Color images available online at www.liebertpub.com/tea
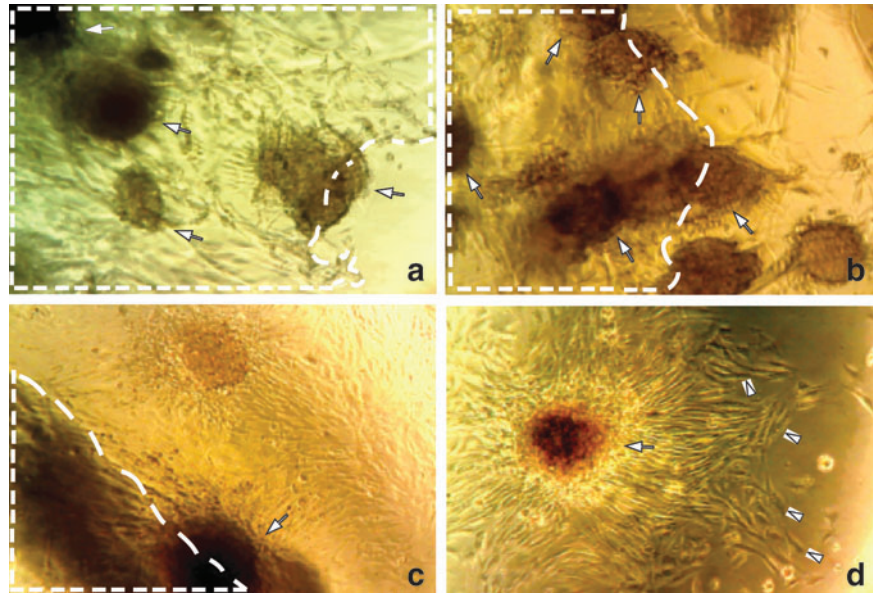
seeded (Fig. 2b), and gradually form into clusters (Fig. 2c). When observed with sequential scanning with confocal microscopy, cells reside not only on the surface of the scaffold but also inside the scaffold for at least $100\,\mu m$ in depth, and on both surfaces of the scaffold. In addition to facilitating cell infiltration, the porous structure is expected to provide a sufficient surface area for seeding significant cell numbers as well as to facilitate the exchange of nutrients and metabolites between seeded cells and the neighboring microenvironment.

To assess cell distribution patterns, scaffolds were modified with RGD peptides and seeded with PMMGFP cells. The cell suspension settled well into the pores of the scaffold within 30 min (Fig. 2b), and after 2 weeks of incubation, cells appeared to be well attached to the scaffold, with an even distribution pattern (Fig. 2c).

Myoblast proliferation and migration out of the scaffold

We next measured cell proliferation on and migration out of the alginate scaffolds. PMMGFP cells were seeded onto the scaffolds as described in the Methods section. The cells absorbed well into the porous scaffold matrix and tended to adhere to each other and grow in clusters (Fig. 3). Over a 3-week observation period, the cells continued to grow in clusters at a high density in the scaffold, as well as to migrate from the scaffold onto the collagen-coated tissue culture plates (Fig. 3).

The cell proliferation rate was calculated by extracting all the viable cells in the scaffold. By the end of 3 weeks, the number of viable cells in the scaffold had expanded from the 0.30×10^6 plated to $\sim 0.81 \times 10^6$ (Fig. 4a), and the cumulative number of cells that had migrated off the scaffold was $\sim 0.11 \times 10^6$ based on cell counts (Fig. 4b). These data indicate that myogenic cells are capable of proliferating and migrating out of the 5% 1LMW:1HMW scaffold at a nearly constant rate during a 3-week period.

IGF-1 release from 5% 1LMW:1HMW scaffolds

The scaffold's potential as a local drug delivery vehicle was tested next. IGF-1 was incorporated into the scaffold by
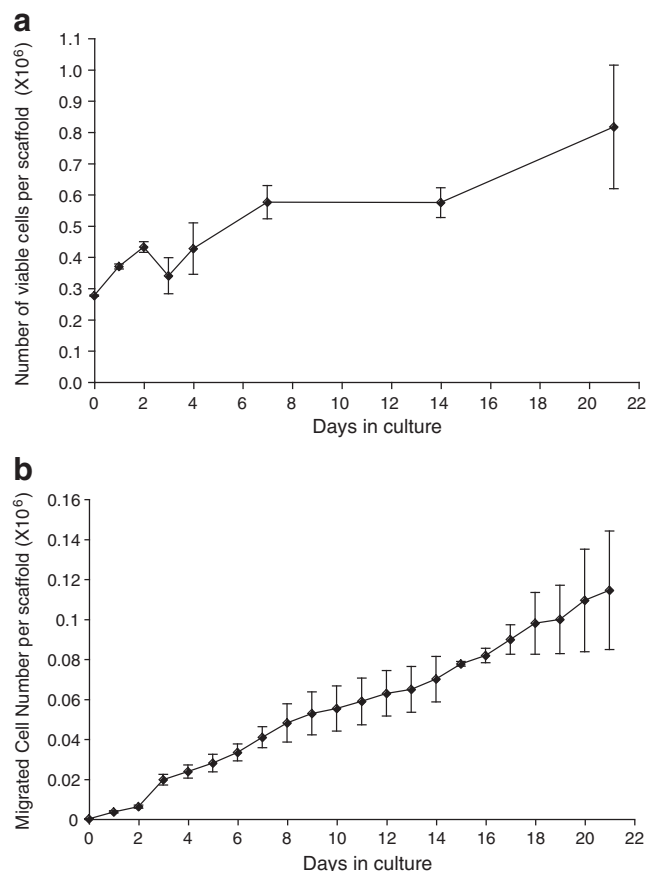

FIG. 4. PMMGFP cells (0.3×10^6) were seeded on the 5% 1LMW:1HMW scaffolds. Myoblasts continued to proliferate over a 3-week period **(a)**. The number of cells growing on the scaffolds was determined by an assay of GFP content. The migration rate of myoblasts off the scaffolds was determined over a 3-week period **(b)**. $n=3$ scaffolds per time point for both proliferation and migration assays; data points are means $\pm$ standard error of the mean.
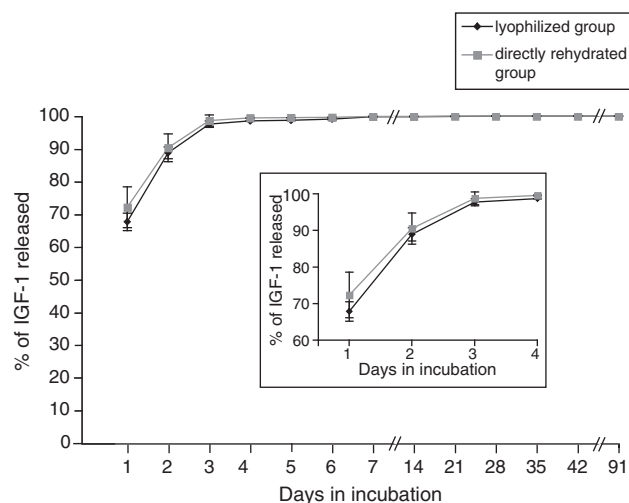
FIG. 5. Insulin-like growth factor-1 (IGF-1) release rate from the 5%1LMW:1HMW scaffolds. The concentration of IGF-1 released from the scaffold at each time point was measured by ELISA, and the total IGF-1 released from the scaffold was plotted as a function of time. $n = 3$ scaffolds per time point; data points are mean±standard error of the mean. Inset is a higher resolution graph of days 1–4.

two methods as described in the Materials and Methods section, and the efficiency of its release from the scaffold was measured. The two methods exhibited similar release patterns, with no significant difference in IGF-1-release kinetics (Fig. 5). Approximately 90% of the IGF-1 was released at a constant rate during the first 3 days (Fig. 5 insert), followed by a sustained slower release rate from day 3 to 14. By day 14, nearly 100% of IGF-1 was released.

Discussion

Results from this study suggest that the 5% oxidized 1LMW:1HMW alginate scaffold that we have designed and fabricated has the desired physical and chemical properties to serve as a favorable synthetic ECM for regenerating skeletal muscle injury. Improvements to previous scaffold models include optimal degradation rate, shape-memory properties for minimally invasive delivery, and favorable surface morphology to support cell and growth factor delivery.

The natural healing process for injured soft tissues such as skeletal muscle typically takes 4–6 weeks, with most of the healing occurring from early week 2 postinjury until the middle of week 5. During this time, implanted scaffolds could serve as a 3D extracellular matrix for cell and growth factor delivery, while at the same time providing space and support for tissue regeneration. As the new muscle tissue is forming and its function is being restored, it would be ideal if the scaffolds slowly degrade, since by the end of the 6-week time frame, the scaffold has served its function and is no longer needed. Degradation of the implanted material during the natural healing time interval would thus eliminate additional surgery to remove the scaffold, as well as reduce the possibility of chronic inflammation caused by the non-degraded material.

By combining oxidization and control over molecular weight distribution of the alginate, we fabricated different types of scaffolds with different degradation properties. Based on the results of *in vitro* degradation experiments, we determined that the 5% oxidized 1:1 LMW:HMW alginate scaffold has the optimal degradation properties that best suit the purpose of *in vivo* skeletal muscle repair, that is, degrades gradually nearly 100% within 6 weeks. The 5% oxidized 1:1 LMW:HMW alginate scaffold was therefore selected for subsequent evaluation.

Beside degradation rate, the scaffolds were characterized for shape-memory properties, which would enable *in vivo* scaffold delivery via a minimally invasive method. The 5% 1:1 LMW:HMW alginate scaffolds possess good shape-memory properties, as after rehydration, they can recover more than 70% of their original volume. In addition, the scaffolds are restored to their original dimensions after compression and rehydration. We expect the dehydrated scaffold to be injected in a compressed state to the site of the muscle damage through a small incision, with a relative ease and accuracy. One method to achieve near simultaneous delivery of scaffold and cells to the injury site would be by use of a double-barrel syringe. In this method, the compressed scaffold is rolled around the outside of a narrow-gauge syringe, and inserted into a larger-gauge catheter. The cell suspension and growth factors are placed inside a syringe, with a blunt needle designed to fit inside the scaffold-containing catheter. The blunt syringe needle is used to push the scaffold into the site of injury, and immediately, the cell suspension/growth factors are injected, resulting in rehydration of the scaffold with the cell suspension *in situ*. This method would deliver cells and growth factors to the scaffold directly and accurately, and restore the scaffold geometry *in vivo* at the site of injury, allowing the scaffold to become a delivery vehicle for cells and growth factors. Such a delivery system has been developed, and studies are underway for its use in muscle repair.

Scaffold surface properties are important features for cell seeding. The surface morphology shown by SEM imaging of a lyophilized scaffold indicates that the scaffold has a porous and interconnected structure. The porosity property confers an appropriate structure for seeding cells, and may also facilitate exchange of nutrients and metabolites within the surrounding *in vivo* microenvironment. In addition, the porosity data indicate that the rehydrated scaffolds have a high water content, which resembles normal muscle tissues.[13]

The 5% 1:1 LMW:HMW scaffold also proved to be a favorable environment for proliferating skeletal muscle cells as shown by its maintenance of cell proliferation and migration *in vitro* during a 3-week period. The proliferation rate of PMMGFP cells on the scaffolds was much slower than their proliferation rate in tissue culture dishes (373-h vs. 24-h doubling time). The retardation of proliferation might be caused by cell attachment characteristics to the scaffold or contact inhibition among cells growing in high density cell clusters.[24,25] However, the proliferation and migration results suggest that the scaffold has reasonable biocompatibility, allowing it to be used as a synthetic extracellular matrix for delivering cells to repair an injured muscle.

According to Boontheekul *et al.*, higher alginate scaffold mechanical properties may increase myoblast functionality such as adhesion, proliferation, and differentiation in a 2D cell culture model, but may lead to different results in a 3D culture.[26] There are varied ways to prepare the scaffolds with

different stiffness,[26] making it possible to test mechanical properties for an ideal material system that is capable of optimizing the appropriate stem cell functionality as well as scaffold degradation. However, a stiffer alginate hydrogel (hydrogel with higher gel mechanical properties) may result in a scaffold with a slower degradation rate, whereas a softer hydrogel (hydrogel with lower gel mechanical properties) may result in a scaffold with a faster degradation rate. As the primary goal for this study was to design a scaffold with an optimal degradation rate (complete degradation within 4–6 weeks required) for the repair of injured skeletal muscle, we chose not to vary matrix stiffness, so that the ideal scaffold degradation rate would not be compromised.

Localized delivery of appropriate growth factors from an implanted scaffold offers the potential to further improve repair of the damaged tissue. The growth factor IGF-1 is known to increase satellite cell proliferation and migration as well as skeletal muscle hypertrophy according to previous studies in a mouse injury model.[27,28] We therefore incorporated IGF-1 into the 5% 1LMW:1HMW alginate scaffold, and measured its release. Nearly 90% of the total IGF-1 was released within the first 3 days, which is a prolonged release if the short half-life of IGF-1 (<30 min *in vivo* [29–31]) is considered. The prolonged release of IGF-1 should maintain its local concentration at a relatively steady level over a 3-day time period, which would be beneficial for regeneration and repair of injured muscle tissue. Moreover, since IGF-1 was largely released within the first 3 days, we anticipate that, when used for *in vivo* treatment of muscle injury, IGF-1 will have an effect on transplanted muscle progenitor cells and host satellite cells in the early stage of the injury recovery process. Satellite cells are activated immediately after an injury as a pulse lasting for only a few days, and since IGF-1 has been demonstrated to stimulate proliferation and migration of satellite cells,[32–35] the early burst release of IGF-1 from the scaffold can be spatially and temporally synchronized with the activation of satellite cells. Upregulation of satellite cell proliferation and migration by IGF-1 may further enhance myogenic cell-mediated skeletal muscle regeneration. The use of the scaffold to deliver growth factors provides the advantage of localized delivery, as growth factors can be targeted to a small region near injury sites. Systemically injected growth factors are often either rapidly taken up by cells, quickly degraded, or bound up by extracellular matrix molecules, all of which cause a rapid decrease in their concentration. Thus, localized delivery would reduce the amount of growth factors needed to achieve the desired effects, which in the current model system is to promote injured muscle tissue regeneration.

These results have clear implications for repair of injured skeletal muscle using a tissue regeneration approach, as we demonstrate the design and fabrication of a biodegradable covalently crosslinked alginate scaffold that can be implanted by a minimally invasive procedure. In addition, long-term survival and migration of cells from within the scaffold coupled with a prolonged growth factor release make this scaffold a promising vehicle for delivery of muscle cells and growth factors *in vivo* to restore the structure and function of injured skeletal muscle as well as other types of tissues. As a next step, the effectiveness of the degradable shape-memory scaffolds will be assessed *in vivo* by implanting it along with myogenic cells and growth factors in a muscle injury model and by comparing the results to bolus injection of cells and growth factors without a scaffold.

Disclosure Statement

No competing financial interests exist.

References

1. Hill, E., Boontheekul, T., and Mooney, D.J. Regulating activation of transplanted cells controls tissue regeneration. Proc Natl Acad Sci U S A **103,** 2494, 2006.
2. Tedesco, F.S., Dellavalle, A., Diaz-Manera, J., Messina, G., and Cossu, G. Repairing skeletal muscle: regenerative potential of skeletal muscle stem cells. J Clin Invest **120,** 11, 2010.
3. Qu, Z., Balkir, L., van Deutekom, J.C., Robbins, P.D., Pruchnic, R., and Huard, J. Development of approaches to improve cell survival in myoblast transfer therapy. J Cell Biol **142,** 1257, 1998.
4. Beauchamp, J.R., Morgan, J.E., Pagel, C.N., and Partridge, T.A. Dynamics of myoblast transplantation reveal a discrete minority of precursors with stem cell-like properties as the myogenic source. J Cell Biol **144,** 1113, 1999.
5. Drury, J.L., and Mooney, D.J. Hydrogels for tissue engineering: scaffold design variables and applications. Biomaterials **24,** 4337, 2003.
6. Bouhadir, K.H., Hausman, D.S., and Mooney, D.J. Synthesis of cross-linked poly(aldehyde guluronate) hydrogels. Polymer **40,** 3575, 1999.
7. Lendlein, A., and Kelch, S. Shape-memory polymers as stimuli-sensitive implant materials. Clin Hemorheol Micro **32,** 105, 2005.
8. Lendlein, A., and Langer, R. Biodegradable, elastic shape-memory polymers for potential biomedical applications. Science **296,** 1673, 2002.
9. Thornton, A.J., Alsberg, E., Albertelli, M., and Mooney, D.J. Shape-defining scaffolds for minimally invasive tissue engineering. Transplantation **77,** 1798, 2004.
10. Thornton, A.J., Alsberg, E., Hill, E.E., and Mooney, D.J. Shape retaining injectable hydrogels for minimally invasive bulking. J Urol **172,** 763, 2004.
11. Gates, C., and Huard, J. Management of skeletal muscle injuries in military personnel. Oper Tech Sports Med **13,** 247, 2005.
12. Kong, H.J., Lee, K.Y., and Mooney, D.J. Decoupling the dependence of rheological/mechanical properties of hydrogels from solids concentration. Polymer **43,** 6239, 2002.
13. Boontheekul, T., Kong, H.J., and Mooney, D.J. Controlling alginate gel degradation utilizing partial oxidation and bimodal molecular weight distribution. Biomaterials **26,** 2455, 2005.
14. Rowley, J.A., Madlambayan, G., and Mooney, D.J. Alginate hydrogels as synthetic extracellular matrix materials. Biomaterials **20,** 45, 1999.

15. Lee, K.Y., Rowley, J.A., Eiselt, P., Moy, E.M., Bouhadir, K.H., and Mooney, D.J. Controlling mechanical and swelling properties of alginate hydrogels independently by cross-linker type and cross-linking density. Macromolecules 33, 4291, 2000.

16. Shapiro, L., and Cohen, S. Novel alginate sponges for cell culture and transplantation. Biomaterials 18, 583, 1997.

17. Eiselt, P., Yeh, J., Latvala, R.K., Shea, L.D., and Mooney, D.J. Porous carriers for biomedical applications based on alginate hydrogels. Biomaterials 21, 1921, 2000.

18. Thorrez, L., Shansky, J., Wang, L., Fast, L., VandenDriessche, T., Chuah, M., Mooney, D., and Vandenburgh, H. Growth, differentiation, transplantation and survival of human skeletal myofibers on biodegradable scaffolds. Biomaterials 29, 75, 2008.

19. Richards, H.A., Halfhill, M.D., Millwood, R.J., and Stewart, C.N. Quantitative GFP fluorescence as an indicator of recombinant protein synthesis in transgenic plants. Plant Cell Rep 22, 117, 2003.

20. Soboleski, M.R., Oaks, J., and Halford, W.P. Green fluorescent protein is a quantitative reporter of gene expression in individual eukaryotic cells. FASEB J 19, 440, 2005.

21. Alshamkhani, A., and Duncan, R. Radioiodination of alginate via covalently-bound tyrosinamide allows monitoring of its fate in-vivo. J Bioactive Compat Polym 10, 4, 1995.

22. Semenov, V.V. Archeological and forensic science biological object search—by using ultraviolet radiation of prescribed energy density and recording phosphorescence signal on colour reversible film. Derwent Innovations Index, Soviet Union, 1989, p. 5.

23. Ikada, Y. Challenges in tissue engineering. J R Soc Interface 3, 589, 2006.

24. Engert, J.C., Berglund, E.B., and Rosenthal, N. Proliferation precedes differentiation in IGF-I-stimulated myogenesis. J Cell Biol 135, 431, 1996.

25. Rosenthal, S.M., and Cheng, Z.Q. Opposing early and late effects of insulin-like growth-factor-i on differentiation and the cell-cycle regulatory retinoblastoma protein in skeletal myoblasts. Proc Natl Acad Sci U S A 92, 10307, 1995.

26. Boontheekul, T., Hill, E.E., Kong, H.J., and Mooney, D.J. Regulating myoblast phenotype through controlled gel stiffness and degradation. Tissue Eng 13, 1431, 2007.

27. Borselli, C., Storrie, H., Benesch-Lee, F., Shvartsman, D., Cezar, C., Lichtman, J.W., Vandenburgh, H.H., and Mooney, D.J. Functional muscle regeneration with combined delivery of angiogenesis and myogenesis factors. Proc Natl Acad Sci U S A 107, 3287.

28. Borselli, C., Cezar, C.A., Shvartsman, D., Vandenburgh, H.H., and Mooney, D.J. The role of multifunctional delivery scaffold in the ability of cultured myoblasts to promote muscle regeneration. Biomaterials 32, 8905, 2011.

29. Guler, H.P., Zapf, J., Schmid, C., and Froesch, E.R. Insulin-like growth factors I and II in healthy man. Estimations of half-lives and production rates. Acta Endocrinol (Copenh) 121, 753, 1989.

30. Lewitt, M.S., Saunders, H., Cooney, G.J., and Baxter, R.C. Effect of human insulin-like growth factor-binding protein-1 on the half-life and action of administered insulin-like growth factor-I in rats. J Endocrinol 136, 253, 1993.

31. Pan, W., and Kastin, A.J. Interactions of IGF-1 with the blood-brain barrier in vivo and in situ. Neuroendocrinology 72, 171, 2000.

32. Charge, S.B.P., and Rudnicki, M.A. Cellular and molecular regulation of muscle regeneration. Physiol Rev 84, 209, 2004.

33. Philippou, A., Halapas, A., Maridaki, M., and Koutsilieris, M. Type I insulin-like growth factor receptor signaling in skeletal muscle regeneration and hypertrophy. J Musculoskelet Neuronal Interact 7, 208, 2007.

34. Adams, G.R. Invited review: autocrine/paracrine IGF-I and skeletal muscle adaptation. J Appl Physiol 93, 1159, 2002.

35. Yang, S.Y., and Goldspink, G. Different roles of the IGF-I Ec peptide (MGF) and mature IGF-I in myoblast proliferation and differentiation. FEBS Lett 522, 156, 2002.

Address correspondence to:
Herman Vandenburgh, Ph.D.
Myomics, Inc.
148 West River St., Suite 1F
Providence, RI 02904

E-mail: hvandenburgh@myomics.com